

Three-dimensional morphology of the *Sinocyclocheilus hyalinus* (Cypriniformes: Cyprinidae) horn based on synchrotron X-ray microtomography

You HE^{1,*}, Xiao-Yong CHEN², Ti-Qao XIAO¹, Jun-Xing YANG^{2,*}

1. Shanghai Synchrotron Radiation Facility, Shanghai Institute of Applied Physics, Chinese Academy of Sciences, Shanghai 201204, China

2. State Key Laboratory of Genetic Resources and Evolution, Kunming Institute of Zoology, Chinese Academy of Sciences, Kunming 650223, China

Abstract: *Sinocyclocheilus* is a cave-dwelling cyprinid genus endemic to southwest China. Several species possess a conspicuous horn on their head, which has been suggested as a constructive troglomorphic trait but lacks substantial evidence. We used non-invasive, high spatial resolution synchrotron X-ray microtomography to investigate the three-dimensional (3D) morphology of the horn of *Sinocyclocheilus hyalinus*, one of eight such troglomorphic species. 3D renderings demonstrated the osteological components, which were comprised of a rear wall comprised of the supraoccipital bone, a remaining frontal wall with numerous fenestrae, and the bottom continuous with the parietal and epiotic. A horn cavity occurred within the horn. The fenestrae in the frontal wall were continuous in the horn cavity and showed elaborate channeling, and were, connected to the cranial cavity by soft tissue. We tentatively called this configuration the “otocornual connection” due to its anatomic and putative functional similarity to the otolateral connection in clupeids and loricariids, which provide an indirect pathway to enhance perception of underwater sound signals. This study provides a functional morphology context for further histological and physiological investigations of such horn structures in *Sinocyclocheilus* cavefish, and we suggest that the horn might enhance acoustic perception to compensate for visual loss in subterranean life, which warrants future physiological examination as lab-reared *S. hyalinus* become available.

Keywords: *Sinocyclocheilus hyalinus*; Cavefish; Horn; Troglomorphism; Synchrotron X-ray microtomography

Abbreviations: C: cerebellum; Cc: cranial cavity; EPO: epiotic; F: frontal; Fo: foramen occipital; Foem: foramen occipital ellipticum magnum; FW: front wall of horn; Hc: horn cavity; LI: inferior lobe; MO: medulla oblongata; M: pd, muscle protractor dorsalis; OP: opercula; ot: optic tectum; P: parital; Pc: pharyngeal cavity; PG: pharyngeal bone; PT: pharyngeal teeth; PTE: pterotic; SO: supraoccipital; TP: tripus; VC: valvula cerebella.

Cyprinid genus *Sinocyclocheilus* is endemic to China with more than 50 valid species (Zhao & Zhang, 2009). All species exhibit cave-dwelling behavior to different degrees. To survive in such extreme subterranean conditions, cavefish have evolved a suite of morphological and physiological characteristics (troglomorphic traits) in both regressive and constructive directions, such as loss of eyes and pigmentation and enhancement of mechanosensory and/or chemosensory perception (Jeffery, 2008; Poulson, 2010; Wilkens, 2003). A sub-group of *Sinocyclocheilus* cavefish possess a conspicuous horn in

their head, which is unique among known cavefish worldwide. The horn has been suggested as a troglomorphic trait but without substantial evidence to support this (Romero et al, 2009). In addition, little is known in regards to its anatomy or function, partially due to the limited availability of such rare specimens. *Sinocyclocheilus hyalinus* Chen, Yang & Zhu (1994), “Tou ming jin xian ba (translucent golden-line barbel)”, is one such horn-containing, anophthalmic troglomorphic species (Chen et al, 1994). It was first reported from two specimens of 87 mm and 83.5 mm standard length, respectively. However, no further research has been

Received: 28 February 2013; Accepted: 12 April 2013

Foundation item: This work was partially supported by the fund of State Key Laboratory of Genetic Resources and Evolution (GREKF13-06)

* Corresponding authors, E-mail: yangjx@mail.kiz.ac.cn; heyou@sinap.ac.cn

reported in the past two decades. X-ray tomography has been applied in large and medium-sized fish osteological studies. The advent of synchrotron X-ray microtomography expands this application into fine structures and soft tissue morphology without any staining in millimeter-centimeter-sized specimens (Pasco-Viel et al, 2010; Boistel et al, 2011). Synchrotron X-rays have the advantage of high coherence suited to phase contrast imaging, an intense photon flux, and a monochromatic and parallel beam with micron/sub-micron spatial resolution.

In the present study, we employed synchrotron X-ray microtomography with 1.85-micron resolution to investigate the horn structure of one specimen of *S. hyalinus*. The resulting three-dimensional (3D) rendering and virtual section revealed the functional morphology of the horn. The resemblance of the horn configuration in the head of *S. hyalinus* and the “otolateralic connection” (such as recessus lateralis) in clupeids (Di Dario, 2004; Grande, 1985; Wilson et al, 2009) and loriciid catfish (Bleckmann et al, 1991; Schaefer & Aquino, 2000) suggest the possibility that the horn in *Sinocyclocheilus* fish might involve the enhancement of acoustic (and/or mechanosensory) perception.

MATERIALS AND METHODS

Specimen

One specimen of *S. hyalinus* measuring 41 mm standard length (Figure 1) was collected in February, 2009 from the Alu Ancient Cave (Luxi County, Yunnan Province), and was preserved in 10% formalin solution for about two years before the experiments. For the experiment, the specimen was switched to 70% ethanol solution and further dehydrated by gradient ethanol. A little shrinkage occurred after dehydration as indicated in the radiography (Figure 1). The horn was situated in the dorsal border between the head and trunk and displayed a forward protrusion.

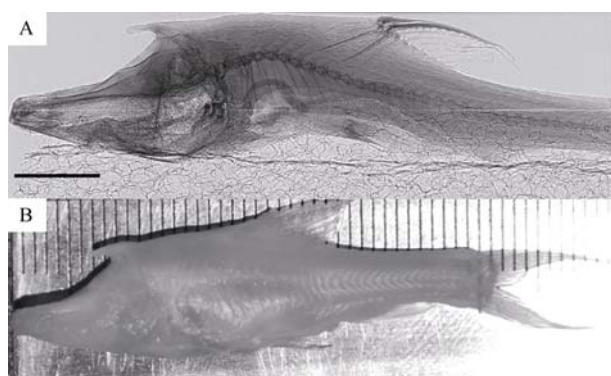


Figure 1 Radiography (A) and photography (B) of the examined specimen of *S. hyalinus*

Scale bar: 5 mm in A. One grid: 1 mm in B.

Synchrotron X-ray microtomography

The experiments were performed at the X-ray imaging beamline (BL13W1) at the Shanghai Synchrotron Radiation Facility (SSRF) in January and February, 2012. The *S. hyalinus* specimen was imaged by monochromatic synchrotron X-ray at 13.0 kV. The X-rays penetrating through the specimen were recorded as two-dimensional (2D) radiograph images (projection) by a charge coupled device (CCD) X-ray camera. The sample-to-detector distance was optimized for obtaining high in-line phase contrast. For synchrotron radiation X-ray microtomography (SR- μ CT) scanning, a PCO.2000 camera coupled with an optical magnification system (PCO AG, Kelheim, Germany) was used. In total, 720 projections, with 2s exposure time for each, were recorded during specimen rotation over 180°. Flat-field images and dark-field images were also collected during each acquisition procedure to correct electronic noise and variations in X-ray source brightness. The data were reconstructed into corresponding slices using the filtered back-projection algorithm (X-TRACT software, CSIRO). The 3D renderings were created from the stack of slices, and were manipulated and analyzed in VG Studio Max (v2.1) software.

During scanning, the specimen was held in a plastic tube vertically mounted on a sample stage. The synchrotron X-ray beam size was 45 mm (width) by 5 mm (height), so a 5 mm high segment including the horn was scanned using the 2X optical objective within the PCO.2000 camera. The local part containing the horn was then scanned using the 4X optical objective covering a height of 3.78 mm. The resulting spatial resolutions were 3.7 micron/pixel and 1.85 micron/pixel, respectively.

Additionally, a 2D radiography of the whole specimen (Figure 1) was stitched by two consecutive radiographies recorded using a VHR1:1 X-ray digital camera with direct coupled (micro) fiber-optic with 9 μ m/pixel resolution (Photonics Science Ltd, Robertsbridge, UK). The specimen was conventionally positioned in soft plastic foam on a sample stage, which vertically moved approximately 5 mm to allow the two consecutive radiographies.

RESULTS

Reconstructed 2D slice and 3D rendering

The original reconstructed slice from the SR- μ CT was an 8-bit grayscale image on the coronal plane. The mineralized tissue (pharyngeal teeth, vertebra, other bones), soft tissue (brain, musculature), and ambient air (cranial cavity, pharyngeal cavity) were easily distinguished from one another according to their different gray values (Figure 2A, C). The mineralized tissues with high grey values were white in the reconstructed slices, whereas air with the lowest value was dark. The 3D rendering was

created in VG Studio software using the stack of slices, from which sagittal and horizontal virtual sections could be further created (Figure 2C). By increasing grey pixel value, the pixel below or equal to the set threshold was interpreted as black. Such manipulation allowed for the

virtual removal of the soft tissue (“virtual corrosion”), and demonstrated the osteological components (Figure 2B, D–I). Areas with the same grey value could be delimited and labeled in designated colors, thus the potential cavity inside the specimen could be labeled.

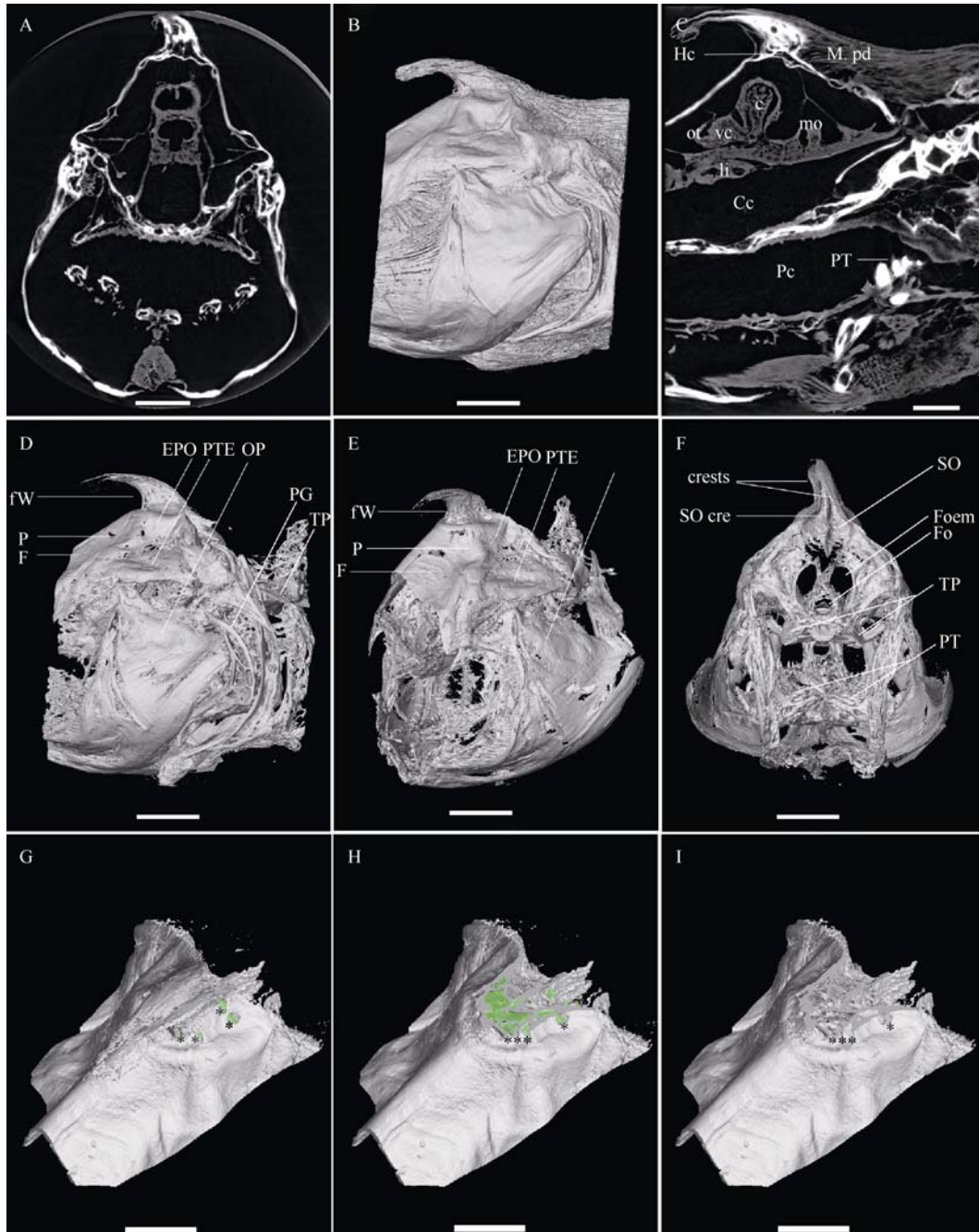


Figure 2 2D reconstructed slices and overall 3D rendering of the horn

Each reconstructed coronal and sagittal slice is presented (A, C), where bones, soft tissue, and air-filled cavities are distinguished from each other by different grey values. Overall 3D rendering (B) was created from the stack of original reconstructed coronal slices. After virtual removal of musculature and other soft tissue, the osteological components are displayed in lateral, oblique, and rear view (D–F). A–F are from SR- μ CT scanning at 3.7-micron resolution. G–I are from scanning at 1.85-micron resolution. The top part of the horn remains in G, but is removed in H and I to display the bony bottom of the horn. The horn cavity is labeled in pale green. H and I differ in whether the remaining horn cavity is labeled or not. A star marks the fenestrae on the frontal wall. Scale bar: 1 mm in A; 1.5 mm in B, D–F; 0.85 mm in C, G–I.

General 3D morphology of the horn

To observe the overall 3D morphology of the horn, a 3D rendering of a 5-mm segment containing the otic region and the horn was created (Figure 2B). The horn was situated at the dorsal otic region of the skull and bent forward as a protrusion with a flattened ending. After virtual removal of musculatures and other soft tissues, the osteological components of the horn were presented, which were divided into rear wall, remaining frontal wall, and bottom. The supraoccipital (SO) bone provided the rear wall (Figure 2F), at which the hypertrophy muscle protractor dorsalis (M.pd) was attached (Figure 2C). The supraoccipital crest and two additional crests on both

sides formed along the suture between the SO and dorsal-posterior parts of the remaining frontal wall (fW) (Figure 2F). The fW, bearing numerous fenestrae, arose from the parietal and epiotic (Figure 2D, E). The bottom was continuous with the parietal and the epiotic, but we were unable to identify whether the parietal or the epiotic formed the bottom. The SO and the fW merged at the distal ending and separated at the basal part of the horn. Thus, a cavity was formed within the horn, and the channeling of the fenestrae in fW connected to it was more elaborate. The horn cavity was labeled in pale green in individual panels (Figures 2 and 3), and further demonstrated the following.

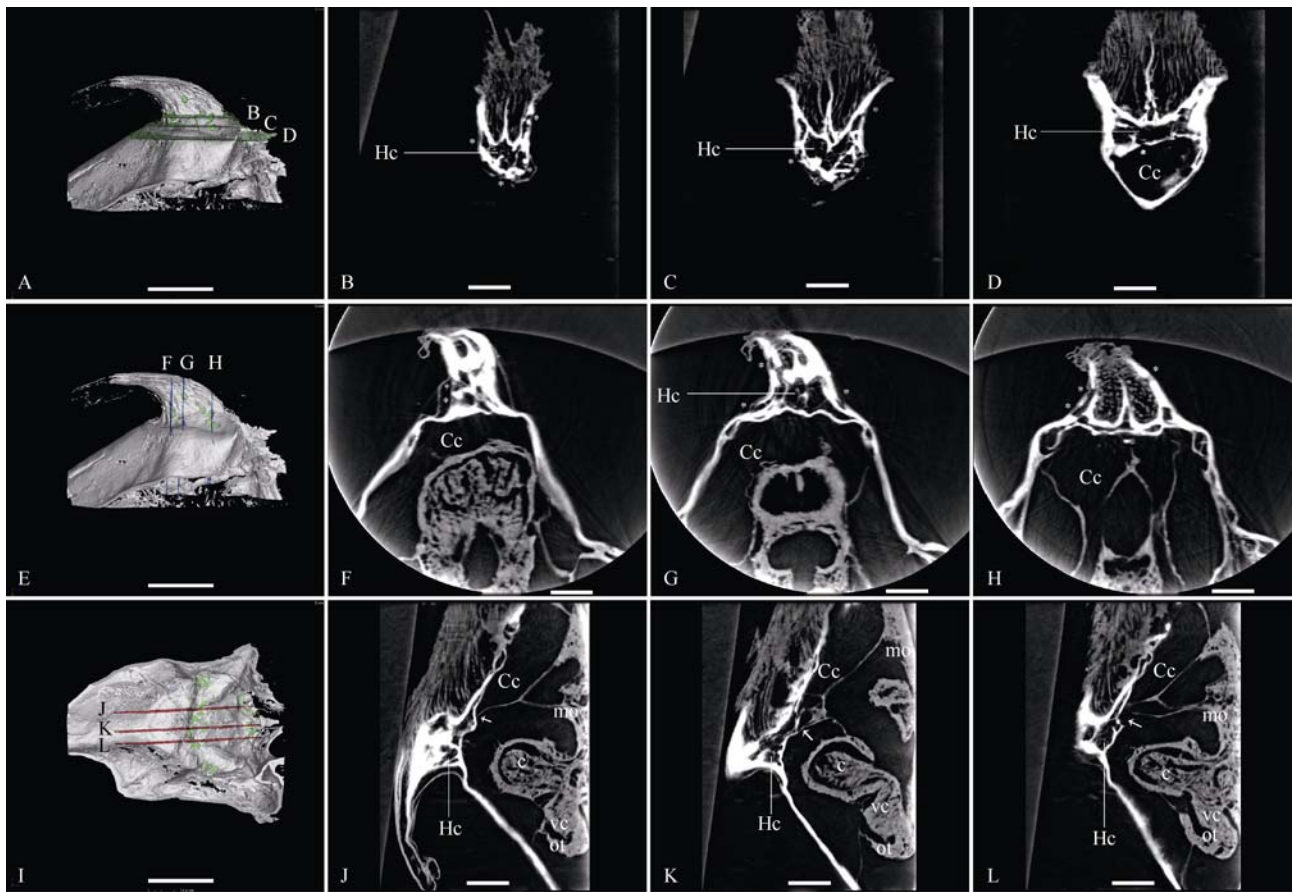


Figure 3 Connecting pathway “frontal wall bearing elaborate fenestrae→horn cavity with soft tissue connection→cranium” revealed in representative horizontal (B–D), coronal (F–H), sagittal (J–L) sections

In the two upper horizontal sections, the horn cavity with trabeculae-like structure and the fenestrae with elaborating channeling are most evident (B, C), while in the lowest horizontal representative section the cranium appears and the bony bottom with one foramen is also shown (D). In the coronal sections, the cranial cavity containing part of cerebellum is evident, and elaborate channeling of fenestrae is also visible (F, G); the horn cavity almost disappears in the posterior representative section (H). The fenestrae and foramen are indicated with a star. In sagittal sections, the soft tissue, which arose from the dorsal medulla oblongata and connected the horn and cranial cavities, are most evident, and the foramen position through which the connection penetrated are indicated by arrows (J–K). Skin tissue investing the horn is also displayed (Figure 3B–D, F, G, J). In each row, the position of the representative sections are indicated in the left most panels, where the horn cavity labelled in pale green is visible through the fenestrae in fW or the foramen in the bony bottom (A, E, I). All images are from SR- μ CT at 1.85-miron resolution. Scale bar: 1.1 mm in A,E, I; 0.55 mm in B–D, J–L; 0.4 mm in F–H.

Configuration of “otocornual connection”

To better demonstrate details, a 3D rendering from an additional SR- μ CT scan at 1.85-micron resolution was created. In the oblique view, the horn cavity from the cranial cavity was evident after removal of the top part of the horn (Figure 2G–I), especially through comparison between the images with and without labeling of the remaining horn cavity (Figure 2H–I). Several foramina in the bony bottom were evident from the ventral view, through which the horn was connected to the cranial cavity (Figure 3I).

Furthermore, sagittal, coronal, and horizontal virtual sections were performed. A configuration, tentatively called the “otocornual connection”, was resolved from these sections. In general, the fenestrae in fW showed elaborate channeling and were continuous with the horn cavity, which in turn was connected with the cranial cavity by soft tissue. The horn cavity and fenestrae with elaborate channeling were most evident in the representative horizontal sections (Figure 3B–D), but were also easily identified in the sagittal and coronal sections where the fenestrae were labeled with a star (Figure 3F, 3G, 3J–L). The soft tissues forming the connection between the horn and cranial cavity were

evident in the representative sagittal sections, which arose from the dorsal medulla oblongata and penetrated into the horn cavity through the bony bottom (indicated by arrows in Figure 3J–L). Unfortunately, we were unable to further identify whether the soft tissue connecting the two cavities was neural or membrane tissue based on the grey value in the image. The trabeculae-like soft tissues (or connective tissue) were also visible in the horn cavity in the horizontal and sagittal sections (Figure 3B, C, K, L). The cerebellum, otic tectum and part of the medulla of the brain with certain decay were also shown in the sagittal sections (Figure 3J–L).

To give an intuitive presentation, two modified 3D renderings were created with the horn cavity labeled in pale green, and the cerebellum and otic tectum labeled in khaki-grey as a reference for the cranium (Figure 4). In one 3D rendering, the encasing structures were set in semitransparent status to emphasize the horn cavity and brain tissue (Figure 4A). In the other rendering, the left half encasing structure was removed to expose the horn cavity and cranium, where the connecting soft tissue was visible and appeared to be membrane rather than fiber tissue (Figure 4B).

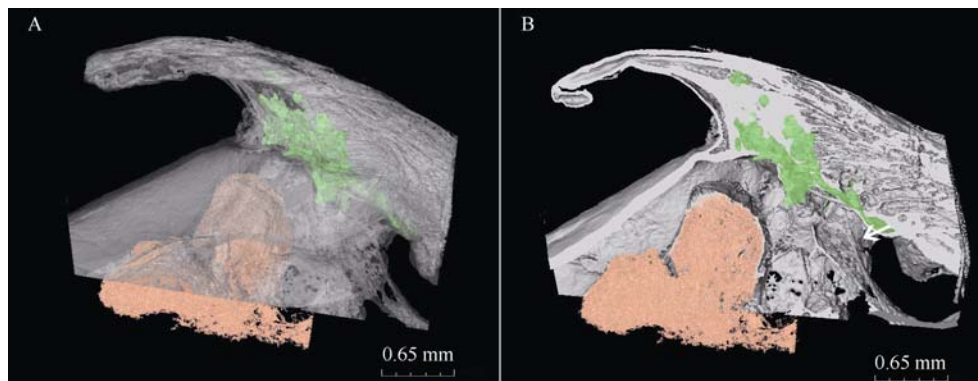


Figure 4 Two 3D renderings for the intuitive presentation of the “otocornual connection” configuration

The horn cavity is labeled pale green, and the cerebellum and otic tectum khaki-grey. The encasing structure is semitransparent in A, whereas the left half encasing structure is removed to expose the horn cavity and cranium in B. The connecting soft tissue is indicated by an arrow in B.

The “otocornual connection” might provide a “frontal wall bearing elaborate fenestrae → horn cavity with soft tissue connection → cranium” pathway, with its potential function discussed in next section.

DISCUSSION

We employed a non-invasive SR- μ CT approach to investigate a *S. hyalinus* specimen at resolution of 1.85-microns, and revealed the osteological components and “otocornual connection” configuration of the horn. The 3D morphology results will help clarify previous reports in relation to anatomic structure, and provide evidence

about the possible function of the horn to enhance acoustic perception to compensate for visual loss in cave life.

The *Sinocyclocheilus* horn is unique among all known cavefish species. Eight troglotrophic species, namely *S. angularis*, *S. aquihornes*, *S. bicornutus*, *S. broadihornes*, *S. furcodorsalis*, *S. hyalinus*, *S. rhinoceros*, and *S. tileihornes*, possess these horny protrusions. Wang et al (1999) delineated the horn of *S. angularis* and *S. bicornutus* as a whole parietal protrusion without supraoccipital or other osteological components, which was concluded in subsequent literature that the horn consisted of the frontal and

parietal bones. Li et al. (2002) performed gross anatomy on *S. rhinoceros* and concluded that the horn was composed of three ossicles set perpendicular to one another. Our 3D morphology results showed that the supraoccipital bone and ossicles arose from the parietal and epiotic, and a bony bottom comprised the osteological base of the horn. These results indicated that the frontal did not build the horn structure, and disagreed with previous findings that the horn is a “whole parietal protrusion”. The explanation that the three ossicles are set perpendicular to one other in *S. rhinoceros* seems to be an incorrect interpretation of the three crests (supraoccipital crest and two additional crests on both sides formed by suture of the supraoccipital and posterior edge of the front wall) found in the rear wall in *S. hyalinus*. Recently, molecular phylogenetic analysis has indicated that all examined horn-possessing species are clustered within one monophyletic clade (Xiao et al, 2005; Li et al, 2008), called the “angularis” clade (Zhao et al, 2009). Systematic investigation of the 3D morphology of horns and analysis of the conservation and variation among them would benefit our understanding of evolution within this “angularis” clade.

The horn has been suggested as a possible troglomorphic characteristic for *Sinocyclocheilus* cavefish (Romero et al, 2009), but whether this structure is related to adapted subterranean life, the function of the horn, and how it contributes to sensory perception are still unknown. From the 3D morphology, it is tempting to speculate that the horn might be an adaptation to enhance acoustic perception. Underwater sound has two physical components, particle motion and sound pressure wave. All fish can detect particle motion through inertial movement between the otolith and sensory epithelia within the inner ear. Some fish can also detect sound pressure by physical connection structures transforming sound pressure into the inner ear (Popper, 1993, 2011). In otophysans, the Weberian ossicles connect the swim bladder and otic capsule. The swim bladder inside the abdominal cavity is set into motion by pressure in the sound field, and such vibrations are transformed by Weberian ossicles into particle motion perceived by the inner ear. In clupeids, the complex *recessus lateralis* structure in the otic region of the skull is an intracranial space into which the supraorbital, infraorbital, preopercular and temporal sensory canals open (Grande, 1985; Di Dario, 2004). A pair of gas-filled auditory bullae in clupeid heads directly contacts the *recessus*

lateralis at the lateral side and the modified utricle at the medial side. Proper configuration of the *recessus lateralis*, auditory bullae and modified utricle provides an indirect pathway for the pressure component of sound to be perceived by the inner ear of certain clupeid species. *Recessus lateralis* lesions or filling auditory bullae with ringer solution has been shown to damage the ability to detect 40 kHz sounds in Gulf menhaden (Wilson et al, 2009). In loriciid, a similar structure is also found in the temporal region of the skull, where a section of the posotic laterosensory canal deep within the ventral layer of the compound pterotic is in direct contact with the horizontal canal of the inner ear (Bleckmann et al, 1991; Schaefer, 2000). These “pressure transducer” otophysical connections in otophysans and otolateral connections in clupeids improve hearing capability (such as auditory sensitivity, frequency bandwidth, and sound source location). In the present 3D rendering of *S. hyalinus* horn, a “frontal wall bearing elaborate fenestrae→horn cavity with soft tissue connection→cranium” configuration was clearly revealed, which was tentatively named the “otocornual connection” due to its anatomical and putative functional similarity to otophysical and otolateral connections, which enhance sound pressure perception. Acoustic perception could be particularly important in the subterranean lightless environment of blind cavefish. Whether the horn functions to enhance acoustic perception warrants future physiological studies as lab-reared *S. hyalinus* become available.

In conclusion, we demonstrated the presence of a cavity inside the horn of *S. hyalinus* with a connection to the cranium. The supraoccipital bone provides the rear wall of the horn, and the remaining frontal wall bears numerous fenestrae. Such a configuration implies a potential putative function as an indirect pathway to perceive sound pressure. This study also provides a functional morphological context for further anatomic and functional investigations of horn structures found in Chinese *Sinocyclocheilus* cavefish.

Acknowledgements: You HE is grateful to Prof. Meeman CHANG (Institute of Vertebrate Paleontology and Paleoanthropology) and Prof. Jiakun SONG (Shanghai Ocean University) for motivating his interest in fish functional morphology. Authors also thank them and Dr. Ning WANG (Institute of Vertebrate Paleontology and Paleoanthropology) for their helpful discussion.

References

- Bleckmann H, Niemann U, Fritzsche B. 1991. Peripheral and central aspects of the acoustic and lateral line system of a bottom dwelling catfish, *Ancistrus sp.* *The Journal of Comparative Neurology*, **314**(3): 452-466.
- Boistel R, Swoger J, Krzic U, Fernandez V, Gillet B, Reynaud EG. 2011. The future of three-dimensional microscopic imaging in marine biology. *Marine Ecology*, **32**(4): 438-452.

- Chen YY, Yang JX, Zhu ZG. 1994. A New fish of the genus *Sinocyclocheilus* from Yunnan with comments on its characteristic adaptation (Cypriniformes: Cyprinidae). *Acta Zootaxonomica Sinica*, **19**(2): 246-253. (in Chinese)
- Di Dario F. 2004. Homology between the *recessus lateralis* and cephalic sensory canals, with the proposition of additional synapomorphies for the Clupeiformes and the Clupeoidei. *Zoological Journal of Linnean Society-Lond*, **141**(2): 257-270.
- Grande L. 1985. Recent and fossil Clupeomorph fish with materials for revision of the subgroups of Clupeoids. *Bulletin of the American Museum of Natural History*, **181**(2): 235-372.
- Jeffery WR. 2008. Emerging model systems in evo-devo: cavefish and microevolution of development. *Evolution and Development*, **10**(3): 265-272.
- Li W, Tao J. 2002. Local dissection of body of the fishes *Sinocyclocheilus rhinoceros*. *Journal of Yunnan Agricultural University*, **17**(3): 207-209. (in Chinese)
- Li ZQ, Guo BC, Li JB, He SP, Chen YY. 2008. Bayesian mixed models and divergence time estimation of Chinese cavefishes (Cyprinidae: *Sinocyclocheilus*). *Chinese Science Bulletin*, **53**(15): 2342-2352.
- Pasco-Viel E, Charles C, Chevret P, Semon M, Tafforeau P, Viriot L, Laudet V. 2010. Evolutionary trends of the pharyngeal dentition in cypriniformes (*Actinopterygii: Ostariophysii*). *PLoS One*, **5**(6): e11293.
- Popper AN, Fay RR. 1993. Sound detection and processing by fish-critical review and major research questions. *Brain Behavior and Evolution*, **41**(1): 14-38.
- Popper AN, Fay RR. 2011. Rethinking sound detection by fishes. *Hearing Research*, **273**(1-2): 25-36.
- Poulson TL. 2010. Cavefish: Retrospective and Prospective. In: Trajano E, Bichuette ME, Kapoor BG. *Biology of Subterranean Fishes*. Enfield: Science Publishers, 1-39.
- Romero A, Zhao YH, Chen XY. 2009. The Hypogean fishes of China. *Environmental Biology of Fishes*, **86**(1): 211-278.
- Schaefer SA, Aquino AE. 2000. Postotic laterosensory canal and pterotic branch homology in catfishes. *Journal of Morphology*, **246**(3): 212-227.
- Wang DD, Chen YY, Li XY. 1999. An analysis on the phylogeny of the genus *Sinocyclocheilus* (Cypriniformes: Cyprinidae). *Acta Academiae Medicinae Zunyi*, **22**(1): 1-6. (in Chinese)
- Wilkens H, Strecker U. 2003. Convergent evolution of the cavefish *Astyanax* (Characidae, Teleostei): genetic evidence from reduced eye-size and pigmentation. *Biological Journal of the Linnean Society*, 2003, **80**(4): 545-554.
- Wilson M, Montie EW, Mann KA, Mann DA. 2009. Ultrasound detection in the Gulf menhaden requires gas-filled bullae and an intact lateral line. *Journal of Experimental Biology*, **212**(21): 3422-3427.
- Xiao H, Chen SY, Liu ZM, Zhang RD, Li WX, Zan RG, Zhang YP. 2005. Molecular phylogeny of *Sinocyclocheilus* (Cypriniformes: Cyprinidae) inferred from mitochondrial DNA sequences. *Molecular Phylogenetics and Evolution*, **36**(1): 67-77.
- Zhao YH, Zhang CG. 2009. *Endemic Fishes of Sinocyclocheilus* (Cypriniformes: Cyprinidae) in China. Beijing: Science Press.